Monthly Notices
of the
ROYAL ASTRONOMICAL SOCIETY

MNRAS **488,** 2650–2657 (2019)
Advance Access publication 2019 July 4

doi:10.1093/mnras/stz1752

A colour-excess extinction map of the southern Galactic disc from the VVV and GLIMPSE surveys

M. Soto,[1★] R. Barbá,[2] D. Minniti,[3,4,5] A. Kunder,[6] D. Majaess,[7,8] J. L. Nilo-Castellón,[2,9] J. Alonso-García,[4,10] G. Leone,[1] L. Morelli,[1] L. Haikala,[1] V. Firpo,[2,11] P. Lucas,[12] J. P. Emerson,[13] C. Moni Bidin,[14] D. Geisler,[2,9,15] R. K. Saito,[16] S. Gurovich,[17] R. Contreras Ramos,[4,18] M. Rejkuba,[19] M. Barbieri,[1] A. Roman-Lopes,[2] M. Hempel,[3,18] M. V. Alonso,[17,20] L. D. Baravalle,[17] J. Borissova,[4,21] R. Kurtev[4,21] and F. Milla[2]

Affiliations are listed at the end of the paper

Accepted 2019 June 13. Received 2019 June 13; in original form 2018 October 19

ABSTRACT

An improved high-resolution and deep A_{K_s} foreground dust extinction map is presented for the Galactic disc area within $295^\circ \lesssim l \lesssim 350^\circ$, $-1.0^\circ \lesssim b \lesssim +1.0^\circ$. At some longitudes the map reaches up to $|b| \sim 2.25^\circ$, for a total of $\sim$148 deg^2. The map was constructed via the Rayleigh–Jeans colour excess (RJCE) technique based on deep near-infrared (NIR) and mid-infrared (MIR) photometry. The new extinction map features a maximum bin size of 1 arcmin, and relies on NIR observations from the Two Micron All-Sky Survey (2MASS) and new data from ESO's Vista Variables in the Vía Láctea (VVV) survey, in concert with MIR observations from the Galactic Legacy Infrared Mid-Plane Survey Extraordinaire. The VVV photometry penetrates $\sim$4 mag fainter than 2MASS, and provides enhanced sampling of the underlying stellar populations in this heavily obscured region. Consequently, the new results supersede existing RJCE maps tied solely to brighter photometry, revealing a systematic underestimation of extinction in prior work that was based on shallower data. The new high-resolution and large-scale extinction map presented here is readily available to the community through a web query interface.

Key words: surveys – Galaxy: disc – Galaxy: stellar content – Galaxy: structure – infrared: stars.

1 INTRODUCTION

Research pertaining to the structure and content of the Milky Way is paramount to understanding the broader Universe. Yet a principal difficulty hindering such efforts is the presence of dense gas and dust along most sightlines. Moreover, dust and gas are inhomogeneous and vary on small scales, thus propagating large uncertainties into low-resolution or magnitude-limited reddening maps, which are used to identify stellar population sequences by enabling the determination of intrinsic colours. Those effects are exacerbated for sightlines towards the Galactic Plane and Centre (Chen et al. 2013).

Consequently, as a result of extinction in part there remains some uncertainty associated with detailing the Galaxy's principal components, such as the disc, bulge, and halo. Over the years considerable effort has been made to solve, or diminish as much as possible, these uncertainties by characterizing the interstellar dust distribution in Galactic extinction maps. Trumpler (1930) was one of the first to try to determine the interstellar light absorption in several Galactic star clusters using spectroscopic techniques. The determination of colour excesses was based on the discrepancy between the expected colour indices, based on stars in the solar neighbourhood, and those actually observed. A major advancement in terms of the reddening maps is the work of Schlegel, Finkbeiner & Davis (1998; henceforth SFD), later superseded by Schlafly & Finkbeiner (2011), which produced an all-sky map based on 100 μm data from *COBE*/DIRBE and *IRAS*. Dust temperature was estimated using the ratio of 100 and 240 μm to trace the column density and derive the extinction by assuming a constant extinction law Rv = 3.1. However, the precision of the map rapidly decreases when approaching high-extinction regions, such as the Galactic Plane (Arce & Goodman 1999; Gonzalez et al. 2012; hereafter G12). This disadvantage limits the use of SFD in Galactic structure studies.

Since extinction is less pronounced at longer wavelengths maps based on infrared data have a comparative advantage over optical

★ E-mail: mario.soto@uda.cl

maps in the bulge and disc. Lada et al. (1994) assumed, based on data of the molecular cloud IC5146, an intrinsic colour range of $0 < (H-K)_0 < 0.3$ for a wide range of spectral types (A0- to M-type stars) to obtain colour excesses with an uncertainty of 2.5 mag, in which was named the near-infrared (NIR) colour excess (NICE) method. This technique was later modified by Lombardi & Alves (2001) by using a combination of 2MASS (Skrutskie et al. 2006) NIR colours $(J-H)$ and $(H-K_S)$ in what they called the NICER (near-infrared colour excess revisited) method. The latter technique was more recently improved by including a variable extinction law in the bulge (V-NICE; Gosling, Bandyopadhyay & Blundell 2009).

Over the last decade, considerable effort has been expended in pursuit of improving the large-scale Galactic extinction maps (e.g. Gonzalez et al. 2011, 2012, 2018; Schultheis et al. 2014). Note that differential reddening will introduce sizeable uncertainties into low-resolution and brightness-limited maps, which we aim to help resolve. Indeed, we can obtain higher resolution through new surveys covering large areas of the sky that provide an opportunity to improve upon previous extinction maps, such as the Two Micron All Sky Survey (2MASS; Skrutskie et al. 2006), the Sloan Digital Sky Survey (York et al. 2000), and the UKIRT Infrared Deep Sky Survey (Lucas et al. 2008). In this study, we will rely on NIR observations from the ESO Visible and Infrared Survey Telescope for Astronomy (VISTA) Variables in the Vía Láctea (VVV) public survey, in concert with mid-infrared (MIR) observations from the Galactic Legacy Infrared Midplane Survey Extraordinaire (GLIMPSE; Benjamin et al. 2005). GLIMPSE is a Legacy programme that used the Infrared Array Camera onboard the *Spitzer Space Telescope* to observe the Galactic Plane in four bands (3.6, 4.5, 5.8, and 8.0) μm.

One of the principal objectives of the VVV Survey (Minniti et al. 2010) is to bolster research of Galactic structure. The VVV survey is one of the initial six ESO VISTA public surveys, and has sampled 562 square degrees of the Milky Way bulge ($-10^\circ < \ell < +10.25^\circ$ and $-10.25^\circ < b < +5^\circ$) and a section of the southern Galactic disc ($-65^\circ < \ell < -10^\circ$ and $-2.25^\circ < b < +2.25^\circ$). The survey has been carried out across five NIR bands (Z, Y, J, H, K_s). The final VVV observations were carried out by 2015 October, completing a variability campaign of 6 yr.

Thus, the area surveyed combined with the filter set used ensures that the VVV has produced among the most detailed maps of the inner Galaxy in the near-infrared domain, providing important data needed to create enhanced extinction maps of our Galaxy. An example of this is the recent discovery of the low-extinction windows in the VVV area (Gonzalez et al. 2018; Minniti et al. 2018).

This study is organized as follows. The data employed to construct the extinction maps are characterized in Section 2, while the Rayleigh–Jeans colour excess method and the construction of our catalogues are described in Section 3. The constructed extinction map and a comparison with previous work are detailed in Section 4. Lastly, our findings are summarized in Section 5.

2 OBSERVATIONS

VVV observations were carried out using the *Visible and Infrared Survey Telescope for Astronomy*, located at the ESO Cerro Paranal Observatory. VISTA is a 4.1 m telescope that is equipped with an Infrared Camera (VIRCAM; Emerson, McPherson & Sutherland 2006; Sutherland et al. 2015), which features an array of 16 2048×2048 pixel^2 Raytheon VIRGO detectors, and a pixel scale of 0.339 arcsec. The VIRCAM has a corrected 1.65 deg diameter field of view, with its detectors arranged in a sparse 4×4 array. There is significant spacing between the detectors, corresponding to 42.5 per cent and 90 per cent of the array size along the x and y axes, respectively. Each VISTA pointing is called a *pawprint*, and covers 0.6 deg^2. For gap-free sky coverage, a set of six offset pointings (known as pawprints) gives one filled rectangular tile. One tile consists of a rectangle of 1.475×1.017 deg^2, with each pixel covered by at least two of the six pawprints, plus two thin stripes each 0.092 deg wide (along the two long edges) covered by one pawprint. In practice, each pawprint is usually comprised of several offset jitter positions for optimal removal of detector artefacts in later processing (Sutherland et al. 2015).

There is overlap between adjacent tiles; within the 562 deg^2 of the complete survey 42 deg^2 is regions where tiles overlapped.

The VVV survey began in 2010, and it is primarily a variability survey with a baseline of over 5 yr. The first year's observations (2010–2011) were carried out in broad-band filters (Z, Y, J, H, K_s), while only K_s observations were planned for the subsequent years (Minniti et al. 2010). Surveys (e.g. VVV) often require dedicated pipelines to reduce the amount of nightly data. The abundance of data associated with NIR surveys, relative to optical campaigns, stems from the need to overcome the instability of IR detectors and the sky brightness compared to stellar sources (Lewis, Irwin & Bunclark 2010). Furthermore, IR sky emission varies over short time-scales, with changes in spatial scale that can be significant. Thus, numerous short exposures are typically obtained to minimize such effects.

The VVV data were reduced using the VISTA data flow system (VDFS) pipeline, which is running at the Cambridge Astronomical Survey Unit (CASU). A detailed account of the CASU pipeline is described in Irwin et al. (2004) and Saito et al. (2012). Briefly, the reduction process consists of a dark subtraction, reset correction, sky background subtraction, destriping correction of a low-level horizontal stripe pattern due to readout noise, jitter stacking of two slightly shifted pawprints to produce a *stacked* pawprint, and tile construction whereby six stacked pawprints are combined. Single-band photometric catalogues are produced for the stacked pawprints and tile images in each field, with zero-point calibrations as described by González-Fernández et al. (2018). The results presented in this work are based on the disc tiles located at $-65^\circ \lesssim l \lesssim -10^\circ$ and $-2.25^\circ \lesssim b \lesssim +2.25^\circ$.

MIR data were obtained through the Infrared Science Archive,[1] which is hosted by the NASA Infrared Processing and Analysis Center, and the observations correspond to the GLIMPSE I (Benjamin et al. 2005) and GLIMPSE II/3D (Churchwell et al. 2009) survey areas overlapping with the VVV campaign.

3 METHOD

The Rayleigh–Jeans colour excess method (Majewski, Zasowski & Nidever 2011; henceforth M11) utilizes near-infrared and mid-infrared photometry, since both sample the Rayleigh–Jeans part of the spectral energy distribution. In that region, stars of diverse spectral types can share almost identical colours, which enables a precise determination of the extinction.

The main advantages of the RJCE method are (1) it provides a colour-excess estimate for each star, and ensures an improved dereddening solution using a colour–magnitude diagram (CMD).

[1] http://irsa.ipac.caltech.edu/cgi-bin/Gator/

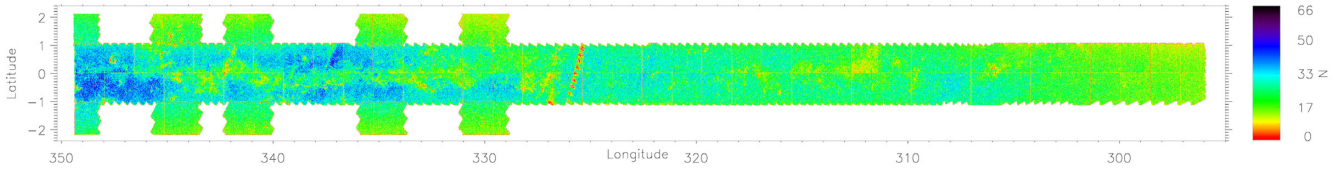

Figure 1. Star count map (1 arcmin × 1 arcmin bin size) for common fields between the VVV and GLIMPSE surveys of the southern Galactic disc.

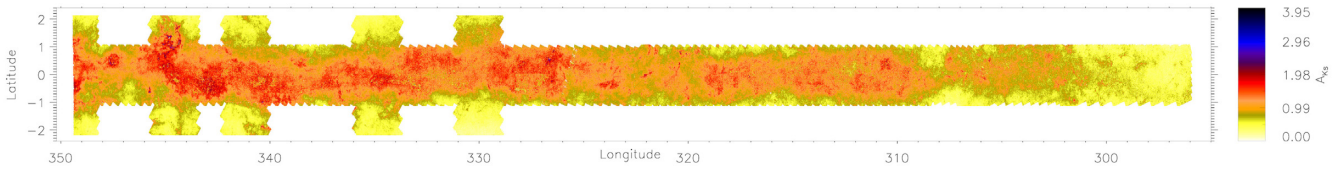

Figure 2. New, improved extinction map constructed by applying the Rayleigh–Jeans colour excess method to the region in Fig. 1.

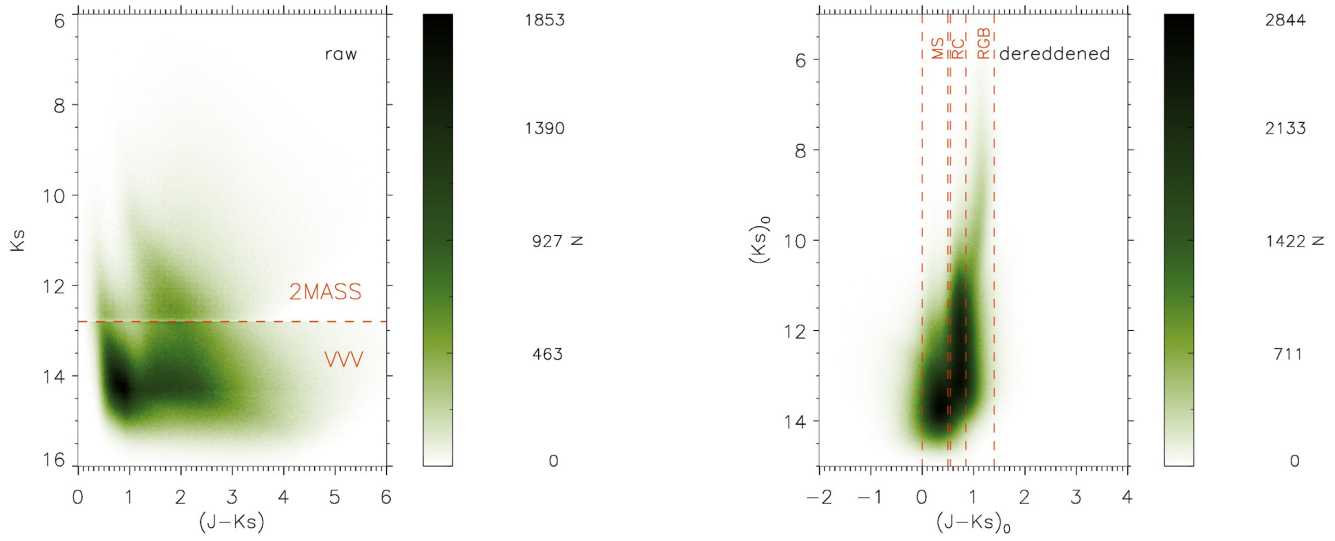

Figure 3. Hess diagrams corresponding to the area of the maps of Figs 1 and 2 and 240 × 400 bins. *Left*: raw CMD, where the VVV magnitudes were transformed to the 2MASS photometric system. Stars with $K_s < 12.8$ (red dashed line) were replaced with photometry from the 2MASS point source catalogue in order to avoid saturation in the VVV catalogues. *Right*: dereddened CMD for the same stars, where the vertical lines highlight the same cuts used in N12 to divide stellar evolutionary phases.

By comparison, other techniques such as NICE (Lada et al. 1994), NICER (Lombardi & Alves 2001), V-NICE (Gosling et al. 2009), or the red clump method of Gonzalez et al. (2011), average or assume intrinsic colours for all stars analysed. Lada et al. (1994) cite a maximum uncertainty for the calculated extinction A_V of 2.5 mag (NICE), as a consequence of the adopted average $(H-K)_0$ colour. (2) The combination of NIR and MIR photometry removes a degeneracy that emerges for methods based solely on NIR colours, where the reddening vector and stellar evolution tracks run nearly parallel for most NIR colour–colour combinations. (3) Variations of the extinction law tend to be less significant for NIR colours (Indebetouw et al. 2005; Zasowski et al. 2009).

The RJCE colour equation cited by M11 and Nidever, Zasowski & Majewski (2012; henceforth N12) is restated below.

$$A(K_s) = 0.918(H - [4.5] - 0.08), \quad (1)$$

where H and [4.5] correspond to a star's magnitude in the 2MASS and GLIMPSE photometric systems. The equation allows for the direct determination of the extinction per star and the construction of extinction maps over extended areas.

3.1 Catalogue construction

To obtain a homogeneous sampling of the underlying stellar populations in the three surveys, a combined catalogue was constructed following the procedure described in detail by Soto et al. (2013). Briefly, the procedure starts by building the photometric transformations on a tile by tile basis that allows us to combine the VVV and 2MASS catalogues: (i) We select the sources in the original CASU catalogues defined as stellar and clean them from detections in close proximity (<2.0 arcsec). (ii) A small matching radius of 0.3 arcsec is then used to combine the VVV resulting list with the 2MASS catalogue using STILTS (Taylor 2006), where only stars with signal-to-noise ratio (SNR) > 7 are used. The resulting combined list VVV–2MASS of isolated stars provides the grounds to calculate linear fits between colours of the two catalogues that will be the photometric transformations. (iii) Multiband VVV JHK_s for tile catalogues of all detections are generated with STILTS, where a maximum offset of 1.0 arcsec to the nearest star is allowed during the matching process. The derived VVV catalogue is then transformed to the 2MASS system using the photometric equations.

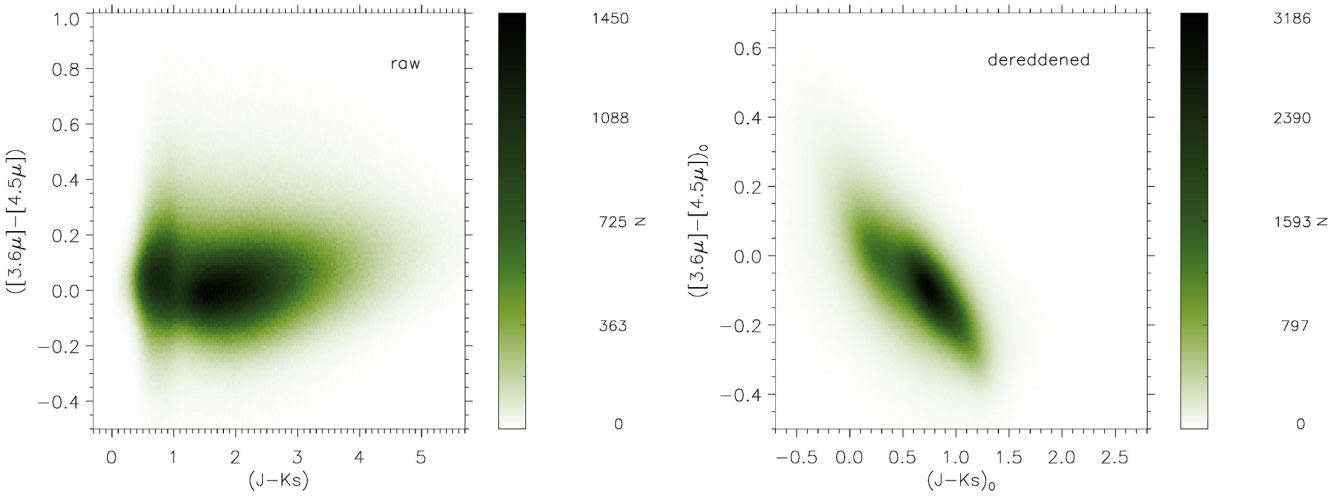

Figure 4. Same as Fig. 3, but for the colour-colour diagrams in ($J - K_s$) and (3.5μ–4.5μ) colours. *Left*: raw (reddened) colour–colour diagram; *right*: dereddened.

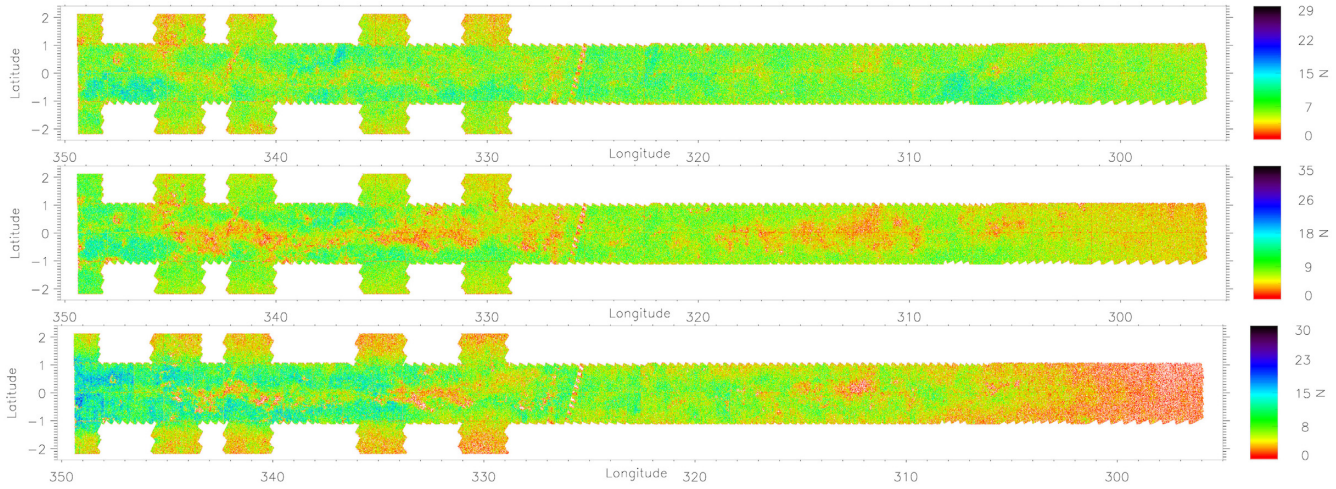

Figure 5. Same as Fig. 1, but divided by stellar populations using the cuts of Fig. 3. *From top to bottom*: star count map for the main sequence, red clump, and RGB, respectively.

It is in this VVV catalogue transformed to the 2MASS photometric system that we replace with 2MASS measurements the magnitudes of stars brighter than $K_s \sim 12.8$ mag, typically saturated in the VVV disc catalogues (see also G12). (iv) At this point we remove all multiple instances of sources from our VVV JHK_s catalogues as detected in the overlap region of the VVV tile edges. A single datum is chosen based on a geometrical criterion, where the source magnitude is selected from the tile furthest from the edge (see also 2MASS; Skrutskie et al. 2006). (v) Finally, the resulting VVV–2MASS catalogue was then cross-referenced to the GLIMPSE MIR photometry using a maximum matching radius of 0.5 arcsec to the nearest source. The final map exhibits a total area of 148 deg^2.

4 RESULTS

The merged 2MASS, VVV, and GLIMPSE stellar density map for the Galactic mid-plane is shown in Fig. 1. The number of stars per resolution element of 1 arcmin ranges from 1 to 66, with the median being 23. The stellar distribution is quite smooth spatially, with only a clear artefact seen as a diagonal strip at $l \sim 328^\circ$ due to a limited number of stars from the GLIMPSE survey. Errors for every pixel in the map were derived from the photometric uncertainties. As expected, the regions closest to the Galactic Centre ($350^\circ \lesssim l \lesssim 340^\circ$) tend to have the highest stellar density.

Fig. 2 displays the generated $A(K_S)$ maps. The extinction decreases precipitously away from the plane, although there exist some highly obscured regions at higher latitudes. Given the RJCE method measures the reddening for each star, in concert with the high density along the plane and the depth of the VVV and GLIMPSE surveys, the resulting reddening map is particularly interesting for studies of highly extincted regions. The extinction results can be retrieved online at the project's webpage.[2]

Figs 3 and 4 convey the RJCE results for the stellar population in the southern Galactic disc, where the VVV fields overlap with the GLIMPSE footprint. The raw IR CMD and colour–colour diagram feature the expected dispersion of stars resulting from

[2]http://www.astro.uda.cl/msoto/extinction/ab.php or http://astro.userena.cl/ExtMapVVV/

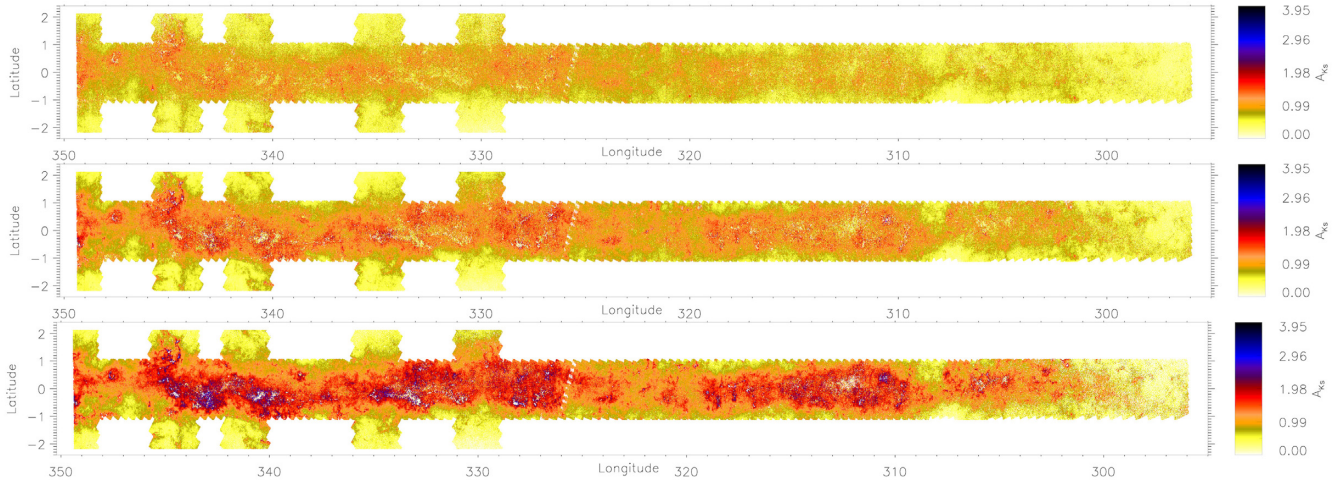

Figure 6. Same as Fig. 2, but discriminating by stellar populations using the cuts of Fig. 3. *From top to bottom*: extinction map for main sequence, red clump, and RGB stars, respectively.

fields with significant differential extinction, such as those near the Galactic Plane. The dereddened CMD displays the same stars, but a narrower sequence is apparent and different stellar populations are distinguishable. In particular, the main sequence (MS), red clump (RC), and red giant branch (RGB) are separable using the $(J - K_S)_0$ colour. The sequences are labelled according to $(J - K_S)_0$ boundaries defined in M11. The run of extinction as a function of distance can be computed, allowing clouds and broader dust complexes to be identified. Similarly, the dereddened colour–colour diagram shows the expected decrease in the dispersion, in agreement with the histograms of selected colour combinations shown in M11 and based on the Girardi et al. (2002) isochrone set.

Fig. 5 features the stellar density of the RGB, RC, and MS populations, whereas Fig. 6 displays the corresponding extinction map.

A comparison of extinction maps made with the RJCE-VVV and other methods now follows and was selected for an area with data common across the different methods. Fig. 7 conveys a comparison with the G12 and N12 extinction maps, in the area corresponding to the VVV bulge field *b238* ($l, b = 7.9°, 0.05°$). The N12 map is based on the RJCE technique applied to 2MASS data and allows options for the population selection: main sequence and turn-off (MSTO), RC, and RGB. The G12 results are tied to a fit of the mean $(J - K_S)$ colour for RC stars, calibrated using the colours of the population endemic to Baade's window. The G12 results were obtained from the BEAM 2 site[3] and translated to A_{Ks} using $A_{Ks} = 0.640 \times E_{(J-K_S)}$. In order to enable a direct pixel-by-pixel comparison, the RJCE-VVV-GLIMPSE extinction map presented here was degraded to match the 2 arcmin resolution of the G12 and N12 maps. Fig. 7 relays the agreement with the N12 map, where the options ALL and PER were selected using Nidever's software[4] (corresponding to the 90th percentile of the total sample of stars irrespective of stellar population in the dereddened CMD). Similarly, the G12 map is also in agreement with the results presented here. A difference exists

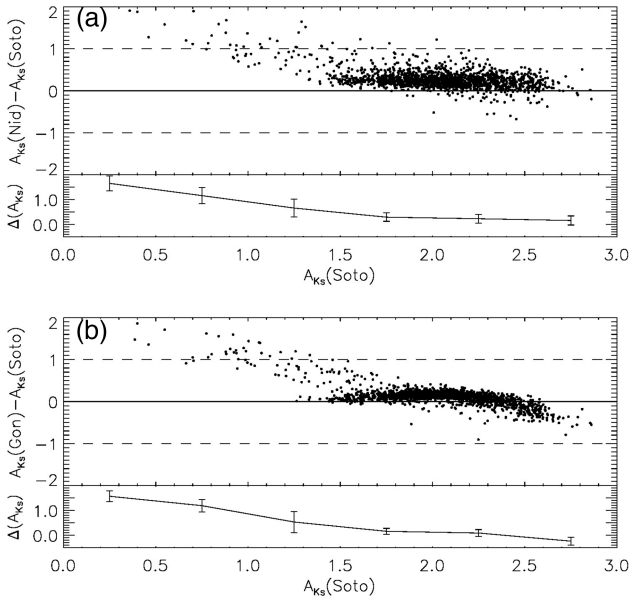

Figure 7. Direct comparison of the extinction per map-pixel in the VVV field b328 $(l, b) = (7.9°, 0.05°)$ derived from this work and compared with the results of (a) N12 and (b) BEAM (G12). A pixel of 2 arcmin × 2 arcmin has been used for consistency.

for a small group of pixels exhibiting $A_{Ks}(Soto) < 1.3$, whereas they appear with higher A_{Ks} in N12 and G12. The difference likely stems from structure around $(l, b) \simeq (352°, -0.3°)$ in the field *b*328. A closer inspection indicates that those pixels with $A_{Ks}(Soto) < 1.3$ in our map are statistically dominated by main-sequence stars (58 per cent of them). The difference relative to G12 emerges because they rely on RC stars to determine extinction, while N12 are restricted by the brighter limit of 2MASS. The 3D extinction map results by Schultheis et al. (2014; henceforth S14) were examined to discern if these low-extinction pixels are present elsewhere. S14 produced a 3D extinction map based on VVV and 2MASS data, and by fitting the M giant temperature–colour and distance–colour

[3] https://www.oagonzalez.net/beam-calculator

[4] Maps and software are currently available at: https://www.noao.edu/noao/staff/dnidever/rjce/extmaps/index.html

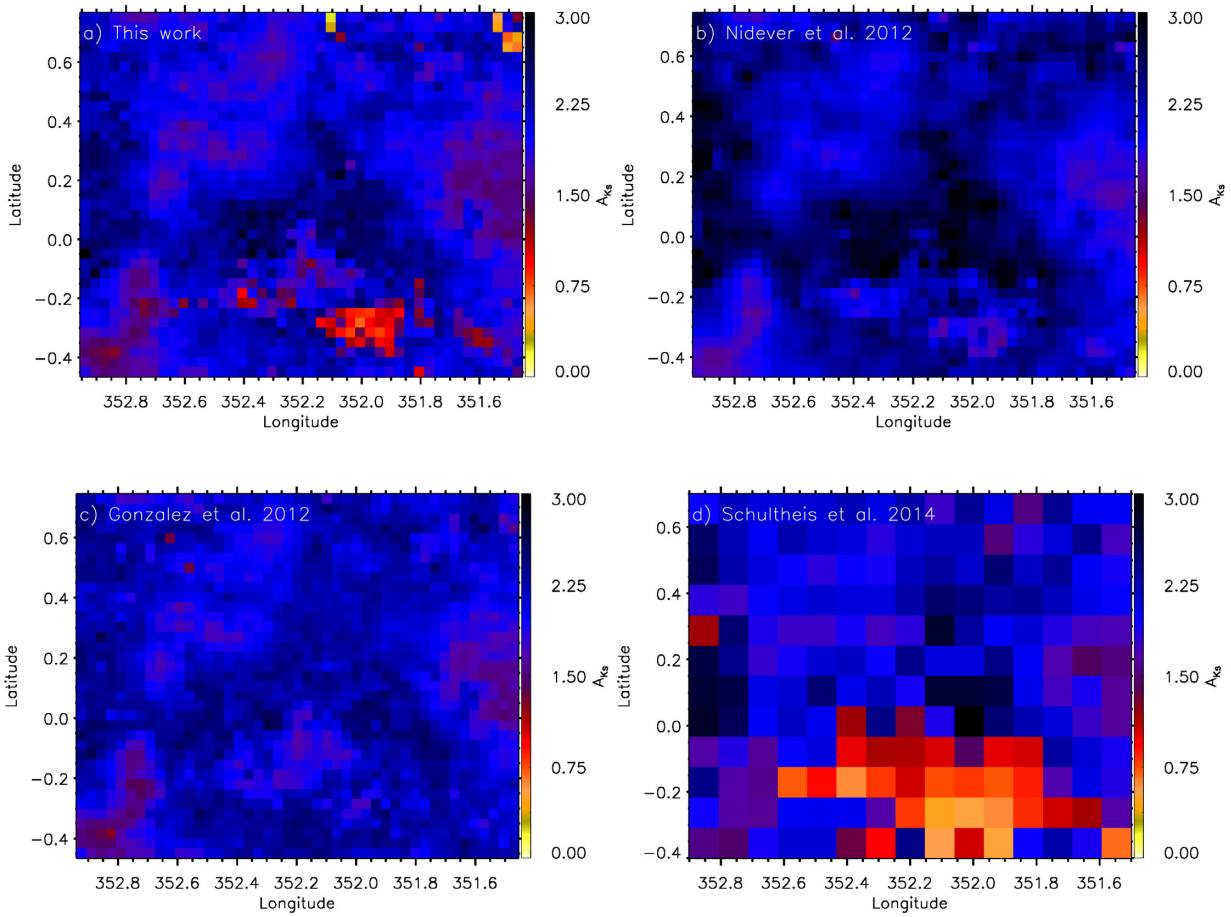

Figure 8. Extinction maps for VVV field *b328*: (a) this work, (b) N12, (c) G12, and (d) S14.

relations to the Besançon model. The result is a 3D extinction map that has been integrated to several distances in the Galactic bulge and is available to the community.[5] Similarly, we find a difference in our results with respect to N12 in the region $(l, b) \simeq (351.5^\circ, 0.65^\circ)$, where a significant fraction of the population on those pixels [48 per cent (36/75)] are MS or highly extincted stars below the faint limit of 2MASS. Thus, the differences found with respect to N12 can be explained by the stars not used in N12 due to the limitations of their data.

Fig. 8 shows the A_{Ks} maps for the VVV field *b*328 in this work, G12, N12, and S14. For the latter, the map was constructed by using the reported A_{Ks} values for an integrated distance of 8 kpc and a 0.1° grid. The corresponding A_{Ks} maps agree, and in particular the same low-extinction zone is present in the S14 map and this work's map $[(l, b) \simeq (352^\circ, -0.3^\circ)]$.

Other possible sources behind the small discrepancies could be related to the photometric colour transformation equations used when developing the maps. This possibility may be explored by reconstructing the full map of the disc using only VVV data with deeper point spread function (PSF) photometry in the future.

Lastly, to further check that the RJCE method performs satisfactorily when tackling a suite of diverse objectives, the approach was applied to deredden a star cluster. Fig. 9 shows a cluster located at Galactic coordinates $l = 328.3^\circ$, $b = -0.60^\circ$ identified by Mercer et al. (2005) using GLIMPSE data. We show the cluster NIR colour image centred in a 0.5° square field, and the respective extinction map as derived from tiles d061 and d062. The dereddened CMD of the same area is likewise shown, where stars in a 1.2 arcmin circle diameter of the cluster centre are highlighted. The cluster stars in the CMD belong primarily to the main sequence, and those in more evolved stages are either foreground targets or bright enough to be visible despite foreground dust. We expect that in the future the approach detailed here can be included in an automated detection routine seeking overdensities in the VVV data, throughout the southern Galactic disc.

5 CONCLUSIONS AND FUTURE WORK

A high-resolution and deep RJCE map is presented here for the southern Galactic disc. The map is based on deep NIR VVV data combined with GLIMPSE, and complemented by 2MASS observations. The maps are consistent with results in the literature, where the main differences partly arise owing to selection effects based on the techniques and data employed. The differences highlight that differential extinction can be found in regions as small as 2 arcmin pixel^{-1} resolution. Never the less, the commonalities found among the maps are reassuring given their semi-independent

[5] http://vizier.cfa.harvard.edu/viz-bin/VizieR?-source=J/A+A/566/A120

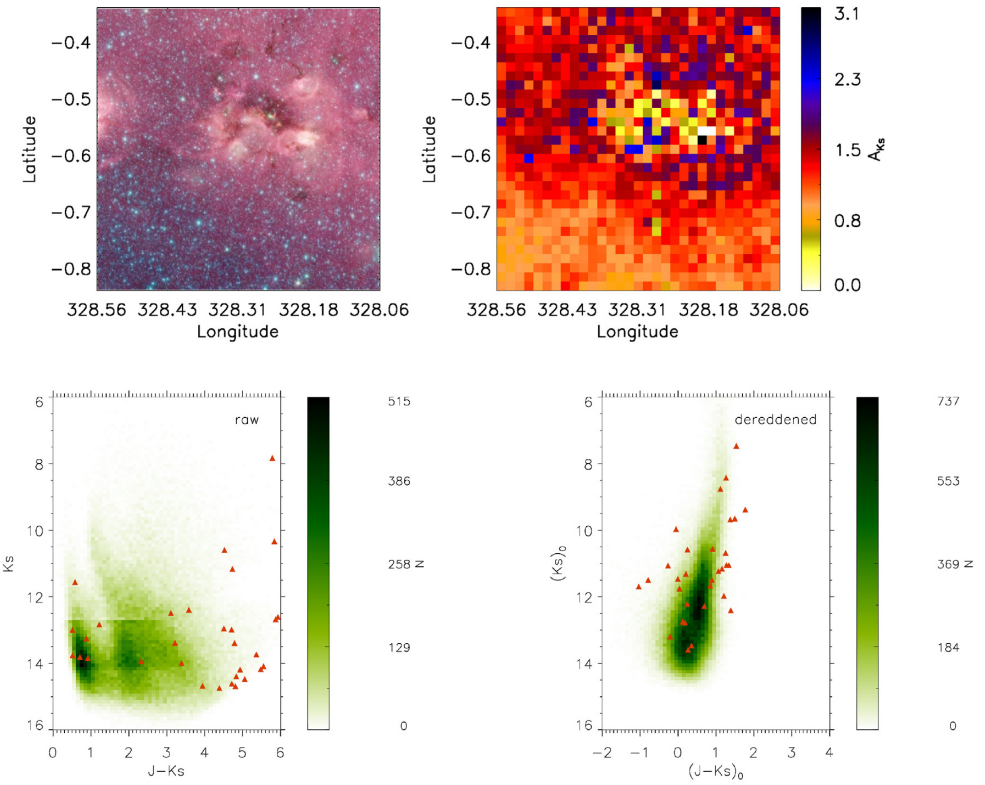

Figure 9. A star cluster in Mercer et al. (2005) discovered using the GLIMPSE point-source catalogue. *Top left*: cut-out of a GLIMPSE mosaic image in a square field with a side of 0.5°. *Top right*: extinction map for the same area which has combined data from tiles *d*061 and *d*062. *Bottom left*: the raw CMD for the selected field where stars within 1.2 arcmin of the cluster centre appear as red triangles and the respective dereddened CMD (*bottom right*).

nature. In the future we plan to improve our maps by replacing the CASU aperture photometry with VVV DoPHOT PSF photometry (Alonso-García et al. 2018). The new photometry will bolster the overall robustness of A_{Ks} by increasing the number of stars per pixel, and enable the maps to rely on VVV NIR data rather than a VVV–2MASS combination. At the same time, we will explore the effects of the variation of the extinction law, which has been set to a constant value in this work, by combining our new results with existing reddening maps obtained with other techniques.

ACKNOWLEDGEMENTS

We would like to thank the anonymous referee for comments and advice that have greatly improved the clarity of the paper. MS acknowledges support from Becas Chile de Postdoctorado en el Extranjero project 74150088. We gratefully acknowledge data from the ESO Public Survey programme ID 179.B-2002 taken with the VISTA telescope, and products from the Cambridge Astronomical Survey Unit (CASU). DM, JB, RK, and JAG gratefully acknowledge support provided by the Ministry for the Economy, Development and Tourism, Programa Iniciativa Cientifica Milenio grant IC120009, awarded to the Millennium Institute of Astrophysics (MAS). DM also acknowledges support from project FONDECYT No. 1170121. DG and DM gratefully acknowledge support provided by the BASAL Center for Astrophysics and Associated Technologies (CATA) through grant AFB-170002. DG also acknowledges financial support from the Direccion de Investigacion y Desarrollo de la Universidad de La Serena through the Programa de Incentivo a la Investigacion de Academicos(PIA-DIDULS). MH gratefully acknowledges support from the BASAL Center for Astrophysics and Associated Technologies (CATA) through grant PFB-06 and Comité Mixto ESO-Gobierno de Chile. RKS acknowledges support from CNPq/Brazil through projects 308968/2016-6 and 421687/2016-9. CMB acknowledges support from FONDECYT regular project 1150060. This material is based upon work supported in part by the National Science Foundation under Grant No. 1066293 and the hospitality of the Aspen Center for Physics. VF acknowledges support from CONICYT Astronomy Program-2015 Research Fellow GEMINI-CONICYT (32RF0002). FM gratefully acknowledges support from Programa DIDULS PT17145. JLNC is also grateful for financial support received from the Programa de Incentivo a la Investigación Académica de la Dirección de Investigación de la Universidad de La Serena (PIA-DIULS), Programa DIULS de Iniciación Científica No. PI 15142. JLNC also acknowledges the financial support from the GRANT PROGRAM N°FA9550-15-1-0167 of the Southern Office of Aerospace Research and development (SOARD), a branch of the Air Force Office of the Scientific Researchs International Office of the United States (AFOSR/IO). This work is based in part on observations made with the Spitzer Space Telescope, and has made use of the NASA/IPAC Infrared Science Archive, which are operated by the Jet Propulsion Laboratory, California Institute of Technology under a contract with NASA. We acknowledge use of

data products from the Two Micron All Sky Survey, a joint project of the University of Massachusetts and the Infrared Processing and Analysis Center/California Institute of Technology, funded by NASA and the NSF.

REFERENCES

Alonso-García J. et al., 2018, A&A, 619, A4
Arce H. G., Goodman A. A., 1999, ApJ, 517, 264
Benjamin R. A. et al., 2005, ApJ, 630, L149
Chen B. Q., Schultheis M., Jiang B. W., Gonzalez O. A., Robin A. C., Rejkuba M., Minniti D., 2013, A&A, 550, A42
Churchwell E. et al., 2009, PASP, 121, 213
Emerson J., McPherson A., Sutherland W., 2006, The Messenger, 126, 41
Girardi L., Bertelli G., Bressan A., Chiosi C., Groenewegen M. A. T., Marigo P., Salasnich B., Weiss A., 2002, A&A, 391, 195
González-Fernández C. et al., 2018, MNRAS, 474, 5459
Gonzalez O. A., Rejkuba M., Minniti D., Zoccali M., Valenti E., Saito R. K., 2011, A&A, 534, L14
Gonzalez O. A., Rejkuba M., Zoccali M., Valenti E., Minniti D., Schultheis M., Tobar R., Chen B., 2012, A&A, 543, A13 (G12)
Gonzalez O. A. et al., 2018, MNRASL, 481, 130
Gosling A. J., Bandyopadhyay R. M., Blundell K. M., 2009, MNRAS, 394, 2247
Indebetouw R. et al., 2005, ApJ, 619, 931
Irwin M. J. et al., in Quinn P. J., Bridger A., eds, 2004, Proc. SPIE Conf. Ser. Vol. 5493, Optimizing Scientific Return for Astronomy through Information Technologies. SPIE, Bellingham, p. 411
Lada C. J., Lada E. A., Clemens D. P., Bally J., 1994, ApJ, 429, 694
Lewis J. R., Irwin M., Bunclark P., 2010, in Mizumoto Y., Morita K.-I., Ohishi M., eds, ASP Conf. Ser. Vol. 434, Astronomical Data Analysis Software and Systems XIX. Astron. Soc. Pac., San Francisco, p. 91
Lombardi M., Alves J., 2001, A&A, 377, 1023
Lucas P. et al., 2008, MNRAS, 391, 136
Majewski S. R., Zasowski G., Nidever D. L., 2011, ApJ, 739, 25 (M11)
Mercer E. P. et al., 2005, ApJ, 635, 560
Minniti D. et al., 2010, New Astron., 15, 433
Minniti D. et al., 2018, A&A, 616, A26
Nidever D. L., Zasowski G., Majewski S. R., 2012, ApJS, 201, 35 (N12)
Saito R. K. et al., 2012, A&A, 537, A107
Schlafly E. F., Finkbeiner D. P., 2011, ApJ, 737, 103
Schlegel D. J., Finkbeiner D. P., Davis M., 1998, ApJ, 500, 525 (SFD)
Schultheis M. et al., 2014, A&A, 566A, 120S (S14)
Skrutskie M. F. et al., 2006, AJ, 131, 1163
Soto M. et al., 2013, A&A, 552, A101
Sutherland W. et al., 2015, A&A, 575, A25
Taylor M. B., 2006, in Gabriel C., Arviset C., Ponz D., Enrique S., eds, ASP Conf. Ser. Vol. 351, Astronomical Data Analysis Software and Systems XV. Astron. Soc. Pac., San Francisco, p. 666
Trumpler R. J., 1930, PASP, 42, 214
York D. G. et al., 2000, AJ, 120, 1579
Zasowski G. et al., 2009, ApJ, 707, 510

SUPPORTING INFORMATION

Supplementary data are available at *MNRAS* online.

Associated to this publication we provide our maps to the public in the websites: http://www.astro.uda.cl/msoto/extinction/ab.php and http://astro.userena.cl/ExtMapVVV/.

Please note: Oxford University Press is not responsible for the content or functionality of any supporting materials supplied by the authors. Any queries (other than missing material) should be directed to the corresponding author for the article.

[1]*Instituto de Astronomía y Ciencias Planetarias, Universidad de Atacama, Copayapu 485, Copiapó, Chile*
[2]*Departamento de Física y Astronomía, Universidad de La Serena, Avenida Juan Cisternas 1200, La Serena, Chile*
[3]*Departamento de Ciencias Físicas, Universidad Andrés Bello, Campus La Casona, Fernández Concha 700, Santiago, Chile*
[4]*Millennium Institute of Astrophysics, Av. Vicuña Mackenna 4860, 782-0436 Macul, Santiago, Chile*
[5]*Vatican Observatory, Vatican City State V-00120, Italy*
[6]*Saint Martin's University, 5000 Abbey Way SE, Lacey, WA 98503, USA*
[7]*Saint Mary's University, Halifax, Nova Scotia, Canada*
[8]*Mount Saint Vincent University, Halifax, Nova Scotia, Canada*
[9]*Instituto de Investigación Multidisciplinario en Ciencia y Tecnología, Universidad de La Serena. Benavente 980, La Serena, Chile*
[10]*Centro de Astronomía (CITEVA), Universidad de Antofagasta, Av. Angamos 601, Antofagasta, Chile*
[11]*Gemini Observatory, Southern Operations Center, La Serena, Chile*
[12]*Centre for Astrophysics Research, Science and Technology Research Institute, University of Hertfordshire, Hatfield AL10 9AB, UK*
[13]*Astronomy Unit, School of Physics and Astronomy, Queen Mary University of London, Mile End Road, London E1 4NS, UK*
[14]*Instituto de Astronomía, Universidad Católica del Norte, Av. Angamos 0610, Antofagasta, Chile*
[15]*Departmento de Astronomía, Universidad de Concepción, Casilla 160-C, Concepción, Chile*
[16]*Departamento de Física, Universidade Federal de Santa Catarina, Trindade 88040-900, Florianópolis, SC, Brazil*
[17]*Instituto de Astronomía Teórica y Experimental (IATE-CONICET), Laprida 854, Córdoba, Argentina*
[18]*Departamento de Astronomía y Astrofísica, Pontificia Universidad Católica de Chile, Vicuña Mackena 4860, Casilla 306, Santiago 22, Chile*
[19]*European Southern Observatory, Karl-Schwarszchild-Str 2, D-85748 Garching bei Muenchen, Germany*
[20]*Observatorio Astronómico de Córdoba, Universidad Nacional de Córdoba, Laprida 854, Córdoba, Argentina*
[21]*Departamento de Física y Astronomía, Facultad de Ciencias, Universidad de Valparaíso, Ave. Gran Bretaña 1111, Playa Ancha, Casilla 5030, Valparaíso, Chile*

This paper has been typeset from a TEX/LATEX file prepared by the author.